

EXPERIMENTAL STUDY ON THE PHASE VELOCITY OF WIND WAVES PART 1: LABORATORY WIND WAVES.

Kuo, Yi-Yu
Hydraulic Civil Engineering, Faculty of Engineering, Kyushu University : Graduate Student

Mitsuyasu, Hisashi
Research Institute for Applied Mechanics, Kyushu University : Professor

Masuda, Akira
Research Institute for Applied Mechanics, Kyushu University : Reserch Associate

<https://doi.org/10.5109/6617922>

出版情報 : Reports of Research Institute for Applied Mechanics. 27 (83), pp.1-19, 1979-07. 九州
大学応用力学研究所
バージョン :
権利関係 :



EXPERIMENTAL STUDY ON THE PHASE VELOCITY OF WIND WAVES

PART 1 LABORATORY WIND WAVES.

By Yi-Yu KUO*, Hisashi MITSUYASU**
and Akira MASUDA***

Wind waves generated in a wind-wave flume are measured with a linear array of wave gauges. The phase velocity and the coherence of the spectral component are determined by a usual technique of the cross-spectral analysis. It is shown that if we consider the effects of the drift current and the angular dispersion of the waves, the linear theory explains well the properties of spectral components in a dominant frequency range ($0.7f_m$ — $1.6f_m$, f_m : spectral peak frequency), where almost all of the wave energy is contained. An explanation is given of the experimental results that the measured phase velocity of the spectral component near the spectral peak shows, in some cases, nearly a constant value.

Key words: Phase velocity, wind wave, spectral component, drift current

1. Introduction

The spectral model is a powerful means for describing ocean waves. In the spectral model for random waves, we generally assume that the wave field is composed of infinitely many free waves propagating independently with the phase velocity given by the small amplitude wave theory. More recently, however, it has been found by many investigators that the phase velocities of spectral components of wind-generated waves do not necessarily follow the linear wave theory. For example, by a new technique for determining the phase velocity of wind waves, Rikiishi (1978) has found that the phase velocity of individual component wave is approximately constant for frequencies near the spectral peak frequency, and the constant value is a little larger than the phase velocity of infinitesimal waves with the spectral

* Graduate Student of Hydraulic Civil Engineering, Faculty of Engineering, Kyushu University.

** Professor, Research Institute for Applied Mechanics, Kyushu University.

*** Research Associate, Research Institute for Applied Mechanics, Kyushu University.

peak frequency. Likewise, Ramamonjaro (1976) and Lake & Yuen (1978) have reported the similar characteristics of the phase velocity of the wind waves. On the basis of these facts found for the phase velocity of the spectral component, several authors (Yifimov et al. 1972, Rikiishi 1978, Toba 1978, Lake & Yuen 1978) have contended that wind-generated waves cannot be satisfactorily decomposed into free waves. Moreover, some authors (Lake & Yuen 1978, Toba 1978) seem to have discarded the linear theory of random waves and attempted to develop some new models to describe the wind-generated waves.

Actually, the wind-generated wave is too complex to be described merely as a linear superposition of free waves, because it is affected by the following factors:

- 1) wind pressure exerted on the wave surface.
- 2) nonlinearity of the wave motion.
- 3) drift current induced by the wind.

First, the effect of the wind pressure is much smaller than that of the other factors and generally can be neglected in studying the phase velocity of wind waves. Secondly, in respect to the nonlinearity of random waves, many theoretical studies have been made, such as generation of forced waves (Tick 1959), energy transfer among wave components (Phillips 1960, Hasselmann 1962) and phase velocity effects (Longuet-Higgins & Philips 1962, Haung 1976, Weber & Barrick 1977). More recently, we have developed a nonlinear theory of random waves, in which both the spectrum of forced waves and the nonlinear dispersion relation are expressed in terms of the spectrum of free waves (Masuda, Kuo & Mitsuyasu 1979, referred to as I). Moreover, we have proposed a method by which to separate each of the spectra of free and forced waves. Quite satisfactory agreements were obtained between the theory developed in I and the experiment on the phase velocity of wind waves in decay area (Mitsuyasu, Kuo & Masuda 1979, referred to as II). On the other hand, the third factor (the drift current) has been investigated by Hidy & Plate (1966), Shemdin (1972), Kato (1974) and others. The studies show that the drift current undoubtedly causes a considerable effect on the wave speed. Particularly, Kato (1974) has developed a theory to evaluate the effect of drift current on the phase velocity of wind waves.

So far, the factors mentioned above have been treated separately with success. In principle, these factors, at least the latter two, should be considered simultaneously in the theoretical model of the wind waves in generation area. However, since this is extremely difficult, we try, as a first step, to study the phase velocity of wind waves within a frame of linear theory by considering the effect of the drift current. According to the previous studies (I and II), drastic effects of the nonlinear forced waves appeared at a frequency region $1.6 f_m \lesssim f$ and the phase velocity in a dominant frequency range $0.7 f_m < f < 1.6 f_m$ could be explained well by the linear

theory. Therefore, the assumptions of the linear theory will be not so large withdrawal as far as the dominant frequency range is concerned, where most of the spectral energy is contained. In fact, it will be shown that, if we consider the effect of the drift current, the linear theory will predict the behaviour of the phase velocity of the spectral component in the dominant frequency range.

2. Laboratory experiment

The measurements were made in a wind-wave flume 13.4 m long, 0.6 m wide and 0.8 m high. Water depth was kept 0.365 m throughout the experiment. Figure 1 shows the experimental arrangement. At a wind blower side of the channel a transition plate with artificial roughness was installed to thicken the boundary layer of the air flow above the water surface. Wind waves generated by the wind propagate in the test section growing gradually and are finally absorbed by the wave absorber at the exhaust section where the width of the flume is widened from 0.6 m to 1 m. The wind speed measured by the Pitot-static tube will be referred to as the reference wind speed U , which corresponds approximately to the mean wind speed in the test section.

Waves were measured by a linear array of twelve wave gauges aligned equidistantly with 4 cm intervals except for the last gauge (Figure 1). Each probe of the wave gauges of resistance-type consists of two platinum wires with a diameter 0.1 mm separated from each other by 2 mm. We had confirmed that the interference among probes was negligible in wave measurement. The linear array of the wave gauges is kept parallel to the longitudinal direction of the flume, and the center of the array corresponds to a fetch of about 8.95 m (Figure 1).

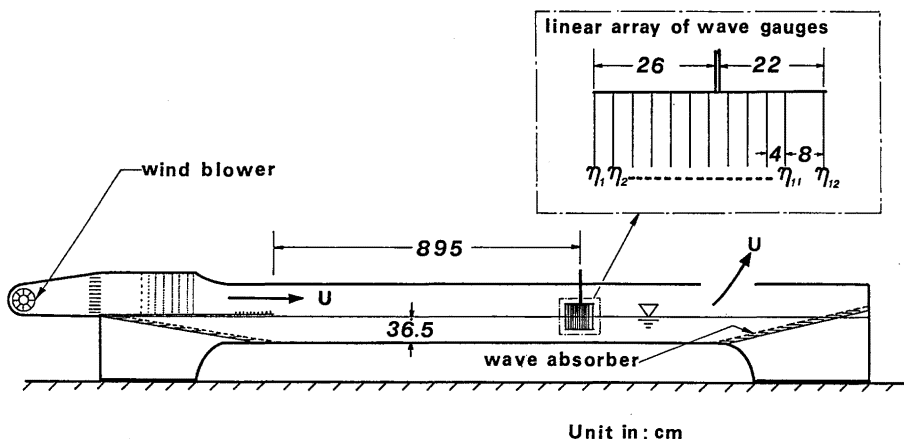


Figure 1, Schematic diagram of wind-wave flume.

Wind with two different speeds U : 7.5 m/s and 10 m/s were used for generating wind waves with different spectral peak frequencies. In both cases, waves were measured continuously for 13 minutes and the wave signals from twelve gauges were recorded simultaneously on an analogue data recorder. In order to use stationary data of the wind wave, we discarded data for the first 3 minutes in the present analysis.

3. Analysis of the wave data

The twelve wave records of each run were digitized simultaneously at sampling frequency 40 Hz. Each of the wave data was divided into ten sub-samples of 51.2 sec, which contained 2048 data points. The spectral analysis of the data was made on a Facom 230-48 computer using a standard program based on fast Fourier transform procedures. In order to calculate the phase velocity of the spectral components, cross-spectra

$$Cr(\omega, l) \equiv CO(\omega, l) - iQU(\omega, l), \quad (1)$$

were computed by using the first wave data η_1 of windward side and the succeeding wave data η_n ($n=2, \dots, 12$). Here, ω is the angular frequency and l is the spacing of two wave gauges. In this way, we could compute the cross-spectra of waves measured at two points of different spacings ($l=4$ cm, 8cm, ...) along the dominant direction of wave propagation. Final data of the cross-spectra were obtained by taking sample mean of ten sub-samples of raw wave spectra and taking moving average of successive seven line spectra. Therefore, equivalent degrees of freedom of the measured spectra are approximately 140.

From the cross-spectra, the phase lag $\bar{\theta}(\omega, l)$, the coherence $\text{Coh}(\omega, l)$, and the phase velocity $C(\omega)$ of the spectral components were determined as

$$\bar{\theta}(\omega, l) = \tan^{-1}[QU(\omega, l)/CO(\omega, l)], \quad (2)$$

$$\text{Coh}(\omega, l) = \{[CO^2(\omega, l) + QU^2(\omega, l)]/\phi_1(\omega)\phi_n(\omega)\}^{1/2}, \quad (3)$$

$$n=2, 3, \dots, 12$$

$$\text{and } C(\omega) = \omega l / \bar{\theta}(\omega, l), \quad (4)$$

where $\phi_n(\omega)$ ($n=2, 3, \dots, 12$) denotes the frequency spectrum at the n -th wave gauge.

4. Experimental results

Typical examples of the measured results for $l=4, 16, 28$ cm are shown in Figures 2 and 3, that correspond to the data for wind speeds of 7.5m/s and 10 m/s respectively. In each figure, from the top to the bottom, power

spectra at two stations, coherence and normalized phase velocity C/C_0 are shown respectively as functions of the normalized frequency f/f_m . Here C_0 is the phase velocity of long-crested linear waves of wave length L in a finite depth h , which is given by

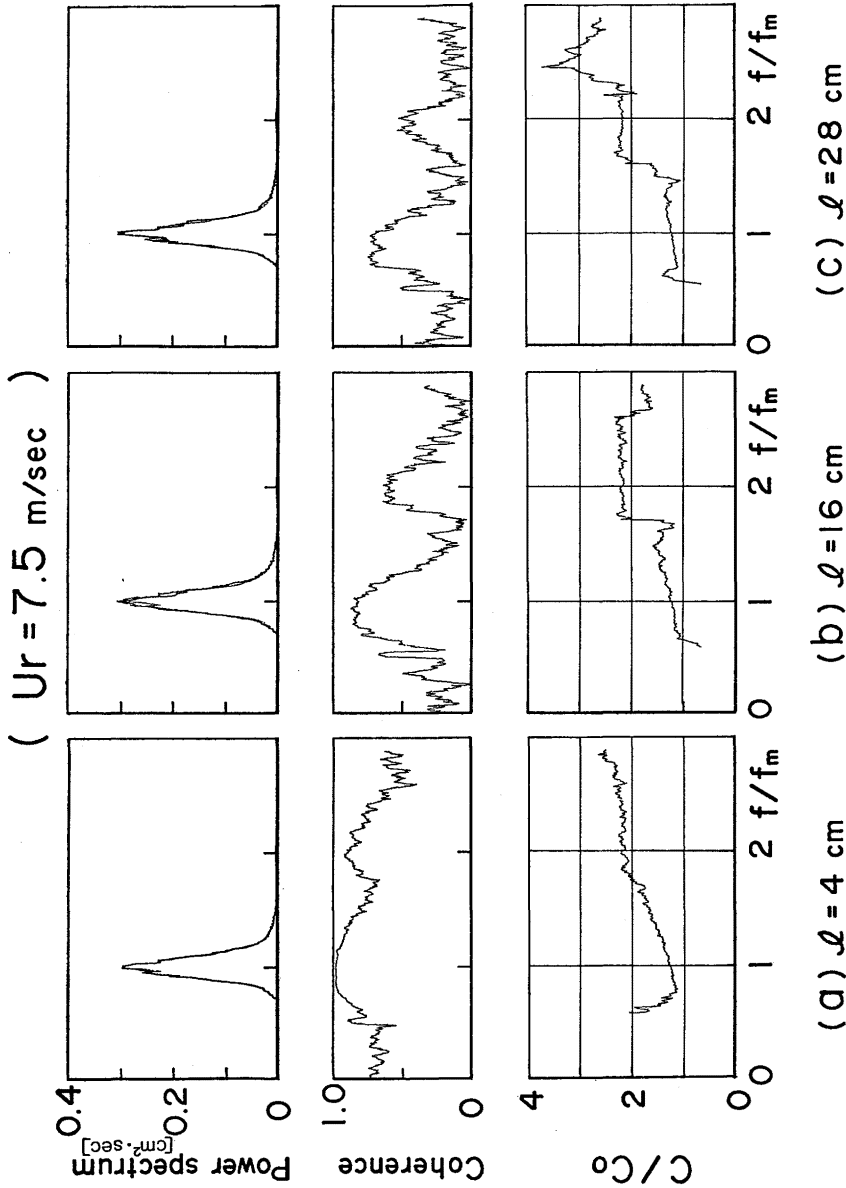


Figure 2, Power spectra, coherence of two wave records, and normalized phase velocity of the spectral components for $U = 7.5 \text{ m/s}$. (a) $k_m L = 12.0$ (b) $k_m L = 48.0$ (c) $k_m L = 84.0$, where $k_m = (2\pi f_m)^2 / g$.

$$C_0(\omega) = \frac{g}{\omega} \tanh\left(\frac{2\pi h}{L}\right), \quad (5)$$

and f_m the spectral peak frequency, which is equal to 3.0Hz for the case of $U=7.5\text{m/s}$ and 2.4Hz for the case of $U=10\text{m/s}$.

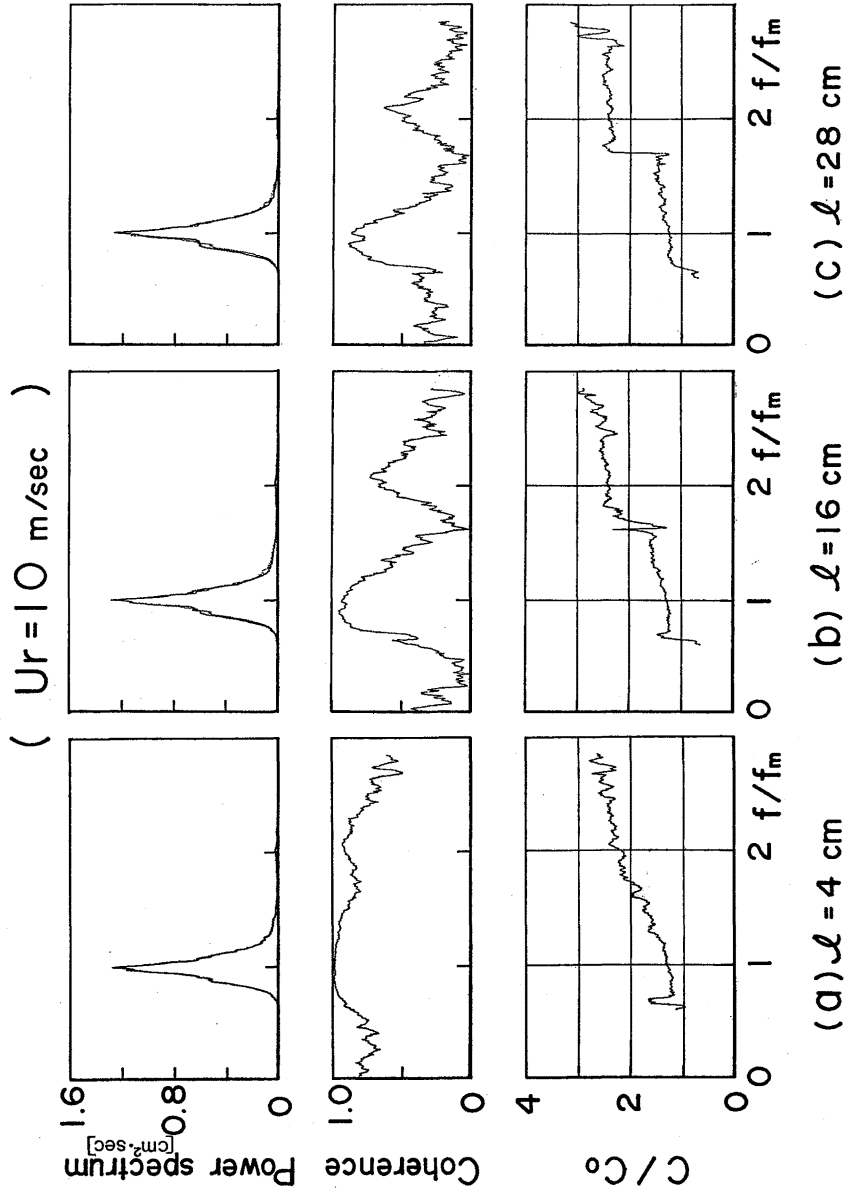


Figure 3, Same as Figure 2 except for $U=10\text{m/s}$. (a) $k_m l=9.6$ (b) $k_m l=38.4$ (c) $k_m l=67.2$

Power spectrum

Generally speaking, spectral forms of laboratory wind waves show high concentration of energy near the spectral peak as compared to those of ocean waves. Figures 2 and 3 show that the energy containing frequency ranges roughly from $0.7 f_m$ to $1.5 f_m$. According to our previous study (Kuo & Mitsuyasu 1978), the spectral form in this frequency range can be represented approximately as

$$\frac{\phi(f)f_m}{E} = \begin{cases} \alpha(f/f_m)^{12} & f < f_m \\ \alpha(f/f_m)^{-12} & f > f_m \end{cases} \quad (6)$$

where E is the total wave energy and α a dimensionless constant taking a value 6.4. As shown in the figures, the power spectra at two stations almost coincide with each other even for the case $l=28$ cm.

The steepness of dominant waves defined by

$$H_{1/3}/L_m = 4\sqrt{E}2\pi f_m^2/g, \quad (7)$$

becomes $1/9.3$ for waves generated by the wind $U=7.5$ m/s and $1/8$ for those generated by the wind $U=10$ m/s.

Coherence

The coherence of the waves measured at two stations is nearly unity for the frequency near the spectral peak frequency f_m so long as the distance between two stations is relatively short (Figures 2a and 3a). However, with the increase of the frequency, the coherence decreases gradually. The minimum coherence can be seen near the frequencies $1.6f_m$. According to our previous study II, these low coherences due to the nonlinear forced waves appear at the frequencies where the spectral densities of the free waves are equal to those of the forced waves (see Appendix). The coherence decreases also with the increase of the distance between two stations. Relations between the coherence and the distance of two stations are shown later in Figure 5 for the case of the frequency component at the spectral peak.

Phase velocity

The normalized phase velocity C/C_0 is larger than unity in the dominant frequency range ($0.7f_m-1.5f_m$) and increases gradually with frequency. In the cases of short distance of wave gauges ($l=4$ cm), the gradual increase of C/C_0 continues up to the frequency near $2f_m$ (Figures 2a and 3a). In the cases of relatively large distance ($l=16$ cm, 28 cm), very sharp increase of

the phase velocity appears at the frequency near $1.6 f_m$ where the coherence shows a minimum value (Figures. 2b, 2c, 3b and 3c). For frequencies near $2 f_m$, the normalized phase velocity C/C_0 is slightly larger than 2.0, almost independent of the frequency.

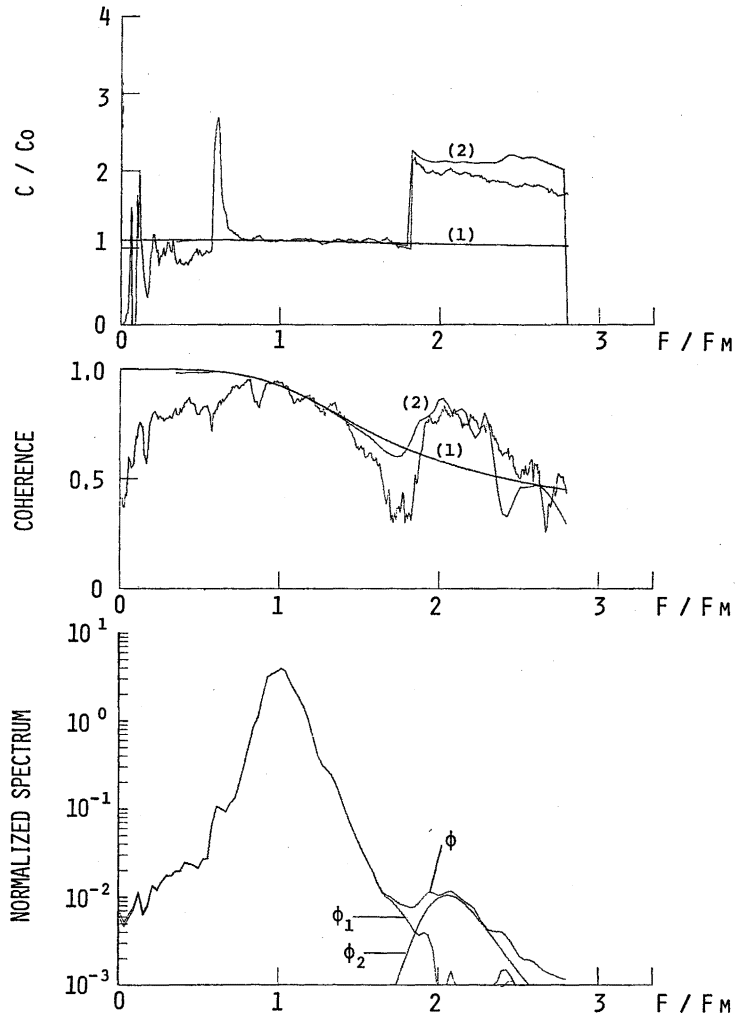


Figure 4, A reproduction of the previous results for wind waves in decay area from II. The observational data for $U=10\text{m/s}$ and $l=12\text{cm}$ ($k_m l=32.4$) are compared with the linear theory (1) and a nonlinear theory to the second-order (2). ϕ_1 and ϕ_2 are the power spectra of free wave and forced wave respectively.

The peculiar behaviour of the phase velocity of wind waves was also found in II, and it was attributed to the effects of nonlinear forced waves. A typical example of the previous results for wind waves in decay area is reproduced in Figure 4. Comparison of Figures 2 and 3 with Figure 4 shows that C/C_0 is generally larger for wind waves in generation area than for those in decay area.

5. Theoretical consideration

For wind waves in decay area, the measured phase velocities of the spectral components in a dominant frequency range ($0.7f_m$ — $1.6f_m$) were very close to the predictions of linear theory, where the effect of angular spreading was taken into account (II). The rapid increase of phase velocity near $1.6f_m$ and corresponding local decrease of the coherence were explained by the contribution from the nonlinear forced waves to cross spectra. The similar phenomena are well expected to occur for wind waves in generation area. In addition to these effects, wind waves in generation area are influenced by the wind stress (wind pressure) and wind-generated current (drift current). As already shown by Kato (1976), the effect of the wind pressure on the phase velocity of wind waves is much smaller than that of the drift current as far as the laboratory wind waves are concerned. Therefore, we neglect the effect of wind pressure and concentrate the discussions on the effects of drift current in the following analysis.

There have been many studies on the velocity profile of the drift current induced by the wind (Shemdin 1972, Dobroklonsky & Liesnikov 1972, and Kato 1974). According to them, the velocity profile of the drift current is given by a logarithmic distribution near the water surface, and its surface velocity U_0 is usually 3% of the mean wind speed (Keulegan 1951, Van Dorn 1953, and Wu 1968).

Although the drift current is much smaller than the phase velocity of ocean waves, it is comparable to the phase velocity of laboratory wind waves. In fact, the value of U_0/C_0 approaches to about 0.5 in the dominant frequency range of the spectrum both for $U=7.5$ m/s and for $U=10$ m/s. Thus, in the investigation of the phase velocity of laboratory wind waves in generation area, we must evaluate the effect of the drift current with logarithmic velocity profile. In the present study, however, comparison is made with a linear model, since it is very difficult to develop a nonlinear theory similar to I under the existence of the drift current. So that, we could not help to confine the analysis to the frequency range $0.7f_m$ — $1.5f_m$, outside of which forced wave components become predominant. Note that the limitation of the analysis to the dominant frequency range makes no serious defects for the practical applications of the results, because almost all of the wave energy, say roughly 90%, is contained in this frequency range.

Phase velocity of wind waves co-existing with the drift current

Kato (1974) has studied the phase velocity of waves in a current with a logarithmic distribution

$$u(z) = U_0 - U_r \ln \frac{z_0 - z}{z_0} - bz, \quad (8)$$

where U_0 is a surface velocity of the drift current, z_0 is a roughness parameter of the water surface, and U_r can be determined from z_0 and U_0 for measured velocity profile as

$$U_r = U_0 / \left\{ \left(1 + \frac{z_0}{h} \right) \ln \left(\frac{h + z_0}{z_0} \right) - \ln \left(\frac{h + z_0}{h/2 + z_0} \right) - 1 \right\}, \quad (9)$$

The last term bz in (8) corresponds to the return flow compensating the surface drift current and b can be determined also from z_0 as

$$b = \frac{2}{h} U_r \ln \left(\frac{h + z_0}{h/2 + z_0} \right), \quad (10)$$

After the perturbation analysis to the second order with respect to a small parameter U_0/C_0 , he showed that his first order solution is sufficiently accurate even for relatively large U_0/C_0 . The first order solution for the phase velocity of waves propagating parallel to the shear flow is given by

$$C = C_0 \left[1 + \frac{U_0}{C_0} \cdot \frac{C_1}{C_0} \right] + \frac{b}{2k} \tanh kh, \quad (11)$$

$$\frac{C_1}{C_0} = 1 + \frac{U_r}{U_0} \left(\frac{Q}{2k \sinh 2kh} - \frac{\tanh kh}{2kz_0} \right), \quad (12)$$

where

$$Q = 2k \left[\frac{\cosh 2kh}{2kz_0} - \frac{1}{y_2} + \sinh y_2 \{ \text{Chi}(y_1) - \text{Chi}(y_2) \} \right. \\ \left. + \cosh y_2 \{ \text{shi}(y_2) - \text{shi}(y_1) \} \right] - \frac{h}{z_0(z_0 + h)}, \quad (13)$$

and

$$y_1 = 2kz_0$$

$$y_2 = 2k(h + z_0)$$

$$\text{shi}(x) = x + \frac{x^3}{3 \cdot 3!} + \frac{x^5}{5 \cdot 5!} + \dots$$

$$\text{chi}(x) = \log |x| + \frac{x^2}{2 \cdot 2!} + \frac{x^4}{4 \cdot 4!} + \dots \quad (14)$$

In (11), the last term of the right hand side is due to the return flow in a wind-wave channel. Its effect on wind-waves is negligible in the present cases.

It should be noted that C can not be determined directly from the angular frequency ω since it is expressed as a function of the wavenumber k . Therefore, we use an iterative method to obtain the wave speed for the assigned frequency ω . That is, the 0-th order wavenumber k_0 is determined by (5) and $C^{(1)}$ is computed by (11) and (12) from k_0 at first, then first order wave number k_1 is determined by $k_1 = \omega/C^{(1)}$, from which $C^{(2)}$ is determined by (11) and (12). Similar procedures are repeated to obtain a consistent value of k . Even for waves propagating obliquely to the shear flow, the same method is applicable if only U_0 is replaced by $U_0 \cos \theta$, where θ is the angle of the wave direction relative to the shear flow. Furthermore, in the above computation, surface velocity of the drift current U_0 and the roughness parameter z_0 are assumed respectively as

$$U_0 = 0.03U, \quad (15)$$

$$z_0 = 0.01. \quad (16)$$

The former relation was mentioned above and the latter is the same to that obtained by Kato (1974) in the similar experimental condition with us.

If the wave number k is determined iteratively, the cross spectrum of waves can be determined by

$$C_r(\omega, l) = \int \phi(\omega) S(\omega, \theta) e^{-ikl \cos \theta} d\theta, \quad (17)$$

where $S(\omega, \theta)$ is an angular distribution function and assumed in this paper as

$$S(\omega, \theta) = \frac{1}{\sqrt{\pi}} \frac{\Gamma(1+m/2)}{\Gamma(1/2+m/2)} \cos^m \theta, \quad (18)$$

where Γ denotes the gamma function.

Figure 5 shows the relation between the coherence of the frequency components at the spectral peak and the spacing of two wave gauges. The distance l to the direction of wave propagation is made non-dimensional by multiplying the wave number k_m . The relations predicted by the linear theory are also shown in the same figure, where the angular distribution function (18) is assumed with $m=2, 4$ and 6 respectively. Figure 5 shows that the angular distribution function $\cos^4 \theta$ fits best to the data both for $U=7.5\text{m/s}$ and for $U=10\text{m/s}$. Therefore we use $m=4$ in the expression (18) to compute the cross spectrum.

In the cases of larger distance between two wave gauges, the effect of nonlinear forced waves on the phase velocity are expected to be relatively small up to a frequency $1.8f_m$ (II). Therefore, we selected the exper-

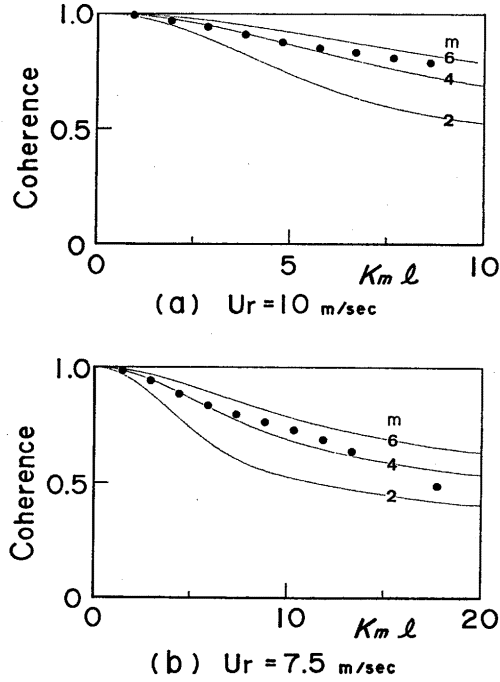


Figure 5, Comparison of the linear theory with the measured coherence at the spectral peak frequency f_m (●). The angular distribution function is assumed as $S(\omega, \theta) \sim \cos^m \theta$, $m=2, 4, 6$ and $k_m l (=2\pi l/L_m)$ is taken as abscissa.

imental data for $l=28$ cm to compare the measured results with the linear theory. The phase velocity and coherence calculated theoretically by the above procedures are compared with the measured values in Figure 6 (a), (b) for wind speeds of 7.5m/s and 10m/s respectively. At the bottom of each figure, a normalized wave spectrum $\phi f_m/E$ is shown.

Figure 6 shows that agreements between the linear theory and the experiment are fairly good, though the agreements for the coherence are confined to the frequency components near f_m and $2f_m$. The agreements for the phase velocity in a dominant frequency range is particularly good for the case of $U=10$ m/s. Although the phase velocity computed for the case of $U=7.5$ m/s is about 10% larger than the measured one, the discrepancy of this order of the magnitude may be possible by the following reasons. First, we did not directly measure the velocity profile, and assumed the formulae (15) and (16) for the flow parameters z_0 and U_0 . Secondly, the determination of the directional distribution was rather indirect. The lack of the exact information on the flow profile and directional distribution

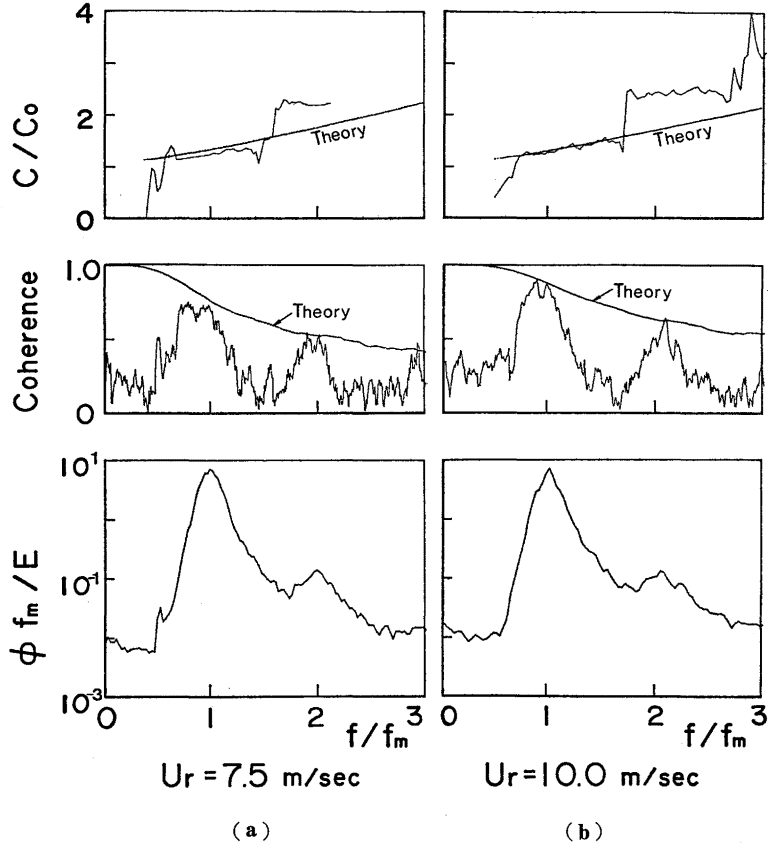


Figure 6, Comparison of the observational results with the linear theory which includes the effects of the drift current and the angular spreading. (a) $U=7.5$ m/s, $k_{ml}=84.0$. (b) $U=10$ m/s, $k_{ml}=67.2$.

inevitably introduces some errors in the estimation of the theoretical phase velocity. If the parameters z_0 , U_0 and m are suitably chosen, much better agreements will be obtained. Indeed, a satisfactory agreement was obtained, though not shown here, by assuming the parameters as $z_0=0.004$, $U_0=0.025U$ and $m=6$. These are permissible values.

With respect to the coherence, large differences between the theory and experiment are found in Figure 6. As expected from II, these differences are attributed to the nonlinear effect, i.e. to the effect of secondary forced waves. The coherence of waves measured at two stations decreases largely when the magnitude of nonlinear forced waves is comparable to that of the free waves (Appendix). Furthermore, the contribution of the nonlinear forced waves in generation area is much larger than that in decay area,

because the wave steepness is much larger in the former than in the latter. Therefore, the frequency range affected by the nonlinear forced waves becomes wider for wind waves in generation area than those in decay area. We need to develop a nonlinear theory for random waves in a shear flow to obtain the better agreements in the coherence. This problem will be studied in near future.

6. Discussion

In this paper we have measured the phase velocity of wind waves in generation area, and compared it with a linear model of random two-dimensional waves in a shear flow, where the dispersion relation found by Kato (1974) was used. Now let us discuss other possible physical factors discarded in the above analysis.

Basically as described in I and II, the wind-wave field is an ensemble of "generalized Stokes waves". That is, wind waves are a random superposition of quasi-linear waves, which have a slightly enlarged phase velocity due to nonlinearity in the sense of Stokes waves and are accompanied with their higher harmonics or, in general, forced waves. This model have succeeded in explaining the phase velocity at least for wind waves in decay area (I and II). Therefore, we must investigate the effects of forced waves and the nonlinear phase velocity.

Wind waves observed in a laboratory have a large wave steepness or a strong nonlinearity, so that appreciable magnitude of forced waves are found for frequencies around $2f_m$. Consequently, it follows that the linear theory of Kato cannot be applied to those frequencies, where forced waves apparently prevail over free waves. In order to evaluate the effects of forced waves on experimentally determined phase velocities for such frequencies, we would have to develop a nonlinear theory analogous to I but under the existence of the drift current.

Here it is to be noted that the phase velocity of the spectral component is determined from the cross spectrum, which depends not only on the physical structure of the wave field but also on an experimental (nonphysical) parameter, i.e. the distance l between two wave gauges. In other words, the cross spectrum and consequent phase velocities are represented through the parameter l . Then, a simple model in the appendix of II shows an important fact that phase velocities are much affected even by small forced-waves, if the spacing l (or kl) is small. To the contrary, for larger spacing, calculated phase velocity depends crucially on which components are larger, free waves or forced waves. To illustrate and verify this situation, Figures 7a and 7b are presented for the cases of $l=4$ cm and 28 cm, respectively, with $U=10$ m/s. The former case indicates that the phase velocities take a nearly constant value in a wide frequency range in agreement with the results of previous investigators (Ramamonjisoa & Coantic

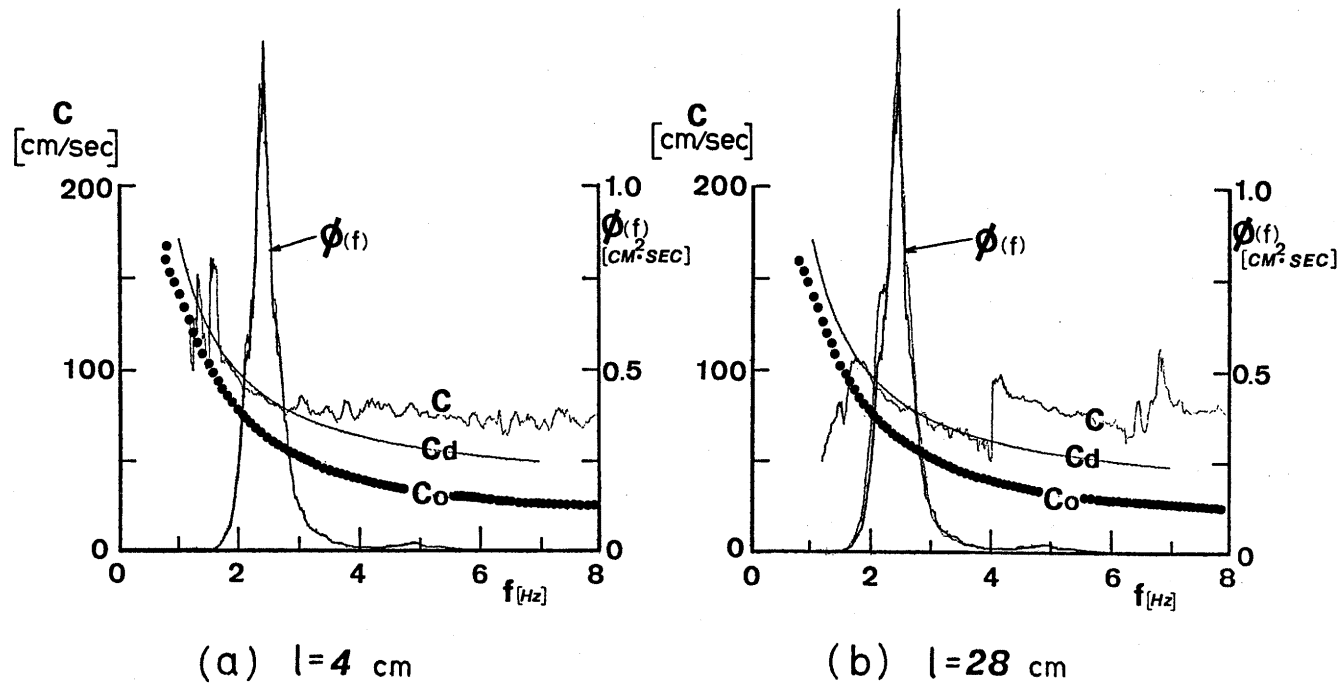


Figure 7, Comparison of the observational data for $U=10$ m/s with the linear theories: linear theory C_0 and the linear theory C_d in which the effects of the drift current and the angular spreading are considered. (a) $k_m l = 9.6$ (b) $k_m l = 67.2$

1976). On the other hand, for the latter case of a large spacing, such a uniform phase velocity cannot be found and a linear theory can explain well the observed behavior of the phase velocity in the frequency range of dominant energy ($0.7f_m$ — $1.6f_m$). Therefore, within the fundamental model described in I and II, we may conclude that an apparent uniform phase velocity in Figure 7a is attributed to the small distance of spacing and that forced waves prevail over free ones for frequencies above $1.6f_m$, where the linear theory cannot hold by no means.

Apart from forced waves, strong nonlinearity in generation area may cause a large increase in the phase velocity of free waves. Indeed, we have shown in II for wind waves in decay area that we cannot neglect such nonlinear effects on the phase velocity when the wave steepness is larger than $1/13$ at least. However, we have given it up to calculate the increase of the phase velocity due to this origin, partly because the third order effect is very hard to evaluate under the existence of the drift current, and partly because the drift current itself is expected to cause a larger increase in the phase velocity than that due to the nonlinear effects.

In conclusion we can state that for wind waves in a laboratory, the measured phase velocity in a dominant frequency range ($0.7f_m$ — $1.5f_m$) follows fairly well the linear theory where the drift current is taken into account.

Wind waves in the ocean, not investigated at all in this paper, are considered not so complex as in a laboratory. For, the wave steepness is too small to produce appreciable magnitude of forced waves or third order increase in phase velocity of free waves. Besides, the drift current becomes less important, since the basic linear phase velocity is so large due to large wavelengths. Therefore, wind waves in the ocean is expected to be explained satisfactorily by the linear theory. We will discuss this subject in another paper.

Acknowledgements

The authors wish to express their gratitude to Mr. T. Honda, Mr. K. Eto and Mr. M. Tanaka for their assistance in the laboratory experiment, and to Miss M. Hojo for typing the manuscript.

References

- 1) Dobroklonsky, S.S. and Lesnikov, B.M.: A study near surface layer of drift currents in laboratory condition, *Izv. Acad. Sci., Atm. Oceanic Physics*, 8 (1972) 1177.
- 2) Haung, N.E. and Tung, C.C.: The dispersion relation for a nonlinear random gravity wave field, *J. Fluid Mech.* 75 (1976) 337.
- 3) Hasselmann, K.: On the nonlinear energy transfer in a gravity-wave spectrum. Part 1. General theory, *J. Fluid Mech.* 12 (1962) 481.
- 4) Hidy, G.M. and Plate, E.J.: Wind action on water standing in a laboratory chan-

- nel, with Appendix by Lilly, D.K., *J. Fluid Mech.* 26 (1966) 651.
- 5) Kato, H.: Calculation of the wave speed for a logarithmic drift current, *Rep. Port & Harbour Res. Inst.* 13 (1974) 3.
- 6) Kato, H., Tsuruya, H., Doi, T. and Miyazaki, Y.: Experimental study of wind waves generated on water currents (2nd report), *Report of Port and Harbour Technical Research Institute*, Vol. 15, No. 4 (1976)
- 7) Keulegan, G.H.: Wind tides in small closed channels, *J. Res. Nat. Bur. Stand.*, Vol. 46 (1951) 358.
- 8) Kuo, Y.Y. and Mitsuyasu, H.: A study of wind-generated waves in decay area, Part 2. On the spectral form of the swell, *Proc. 25-th Conference of the Coastal Engineering* (1978) 48 (in Japanese)
- 9) Longuet-Higgins, M.S. and Phillips, O.M.: Phase velocity effects in tertiary wave interaction, *J. Fluid Mech.* 12 (1962) 333.
- 10) Lake, B.M. and Yuen, H.: A new model for non-linear wind waves, Part 1, Physical model and experimental evidence, *J. Fluid Mech.* 88 (1978) 33.
- 11) Masuda, A., Kuo, Y.Y. and Mitsuyasu, H.: On the dispersion relation of random gravity waves, Part 1, Theoretical framework, *J. Fluid Mech.* 92 (1979) 731.
- 12) Mitsuyasu, H., Kuo, Y.Y. and Masuda, A.: On the dispersion relation of random gravity waves, Part 2, An Experiment, *J. Fluid Mech.* 92 (1979) 745.
- 13) Phillips, O.M.: On the dynamics of unsteady gravity waves of finite amplitude, Part 1, The elementary interaction, *J. Fluid Mech.* 9 (1960) 193.
- 14) Ramamonjiarisoa, A. & Coantic, M.: Loi experimentale de dispersion des vagues produites par le vent sur une faible longueur d'action, *C.r. hebdomadaire Séances Acad. Sci. Paris B* 282 (1976) 111.
- 15) Rikiishi, K.: A new method for measuring the directional wave spectrum, Part II, Measurement of the directional spectrum and phase velocity of laboratory wind waves, *J. Phys. Oceanogr.* 8 (1978) 518.
- 16) Shemdin, O.H.: Wind-generated current and phase speed of wind waves, *J. Phys. Oceanogr.*, 2 (1972) 411.
- 17) Tick, L.J.: A non-linear random model of gravity waves I, *J. Math. Mech.* 8 (1959) 643.
- 18) Toba, Y.: Stochastic form of the growth of wind waves in a single-parameter representation with physical implications, *J. Phys. Oceanogr.* 8 (1978) 494.
- 19) Van Dorn, W.G.: Wind Stress on an artificial pond, *J. Marine Res.* 12 (1953) 249.
- 20) Weber, B.L. and Barrick, D.E.: On the nonlinear theory for gravity waves on the ocean's surface, Part I, Derivations, *J. Phys. Oceanogr.* 7 (1977) 3.
- 21) Wu, J.: Laboratory studies of wind-wave interactions, *J. Fluid Mech.* 34 (1968) 91.
- 22) Yefimov, V.V., Solov'yev, Yu.P. and Khristoforov, G.N.: Observational determination of the phase velocities of spectral components of wind waves, *Izv. Atmos. Oceanic Phys.* 8 (1972) 435.

(Received May 8, 1979)

Appendix

Let us consider the random wave field of the form

$$\eta(x, t) = A(\omega) \exp\left\{\frac{\omega^2}{g}x - \omega t\right\} + B(\omega) \exp\left\{\frac{\omega^2}{2g}x - \omega t\right\}, \quad (\text{A-1})$$

where A and B are uncorrelated random amplitudes of free wave and forced wave respectively. The model is the same to that in the appendix of II. The first term corresponds to the free wave and the second to the second harmonics of the other free wave

$$A\left(-\frac{\omega}{2}\right) \exp\left\{\frac{1}{g}\left(\frac{\omega}{2}\right)^2 x - \left(\frac{\omega}{2}\right)t\right\}, \quad (\text{A-2})$$

which propagates twice as fast as the first free wave. Since A and B are uncorrelated, i. e. $\langle A(\omega)B(\omega) \rangle = 0$, the cross spectrum of wave data $\eta(o, t)$ and $\eta(l, t)$ is given by

$$\begin{aligned} CO(\omega, l) - iQU(\omega, l) &= (\langle A^2(\omega) \rangle \cos \frac{\omega^2}{g}l + \langle B^2(\omega) \rangle \cos \frac{\omega^2}{2g}l) \\ &\quad - i(\langle A^2(\omega) \rangle \sin \frac{\omega^2}{g}l + \langle B^2(\omega) \rangle \sin \frac{\omega^2}{2g}l). \end{aligned} \quad (\text{A-3})$$

From the cross spectrum, we can determine the coherence Coh as

$$\text{Coh}(\omega, l) = \frac{\left\{1 + a^2 + 2a \cos\left(\frac{\omega^2}{2g}l\right)\right\}^{1/2}}{1 + a}, \quad (\text{A-4})$$

where a is the ratio of the forced wave energy $\langle B^2 \rangle$ to the free wave energy $\langle A^2 \rangle$

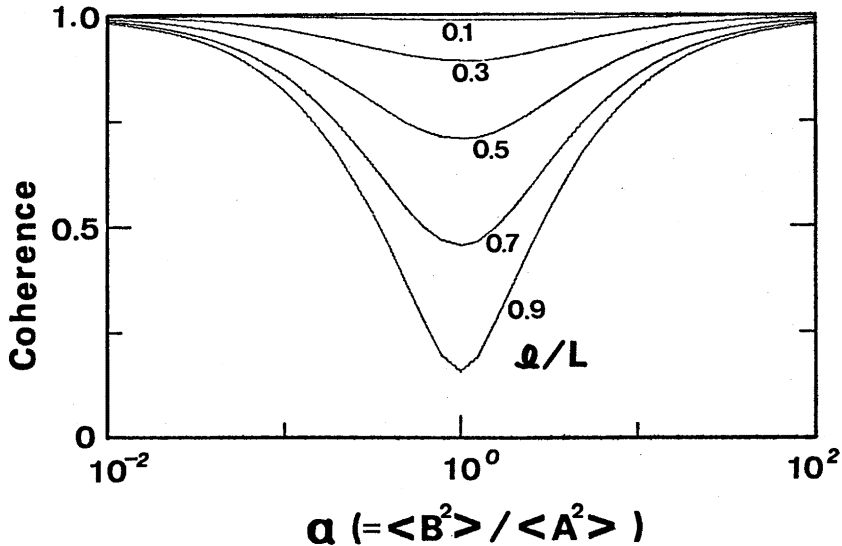


Figure A-1 The relation between Coh and $a = \langle B^2 \rangle / \langle A^2 \rangle$

at fixed ω .

The relation between Coh and a given by (A-4) are shown in Figure A-1, where a relative spacing $l/L (= \omega^2 l / 2\pi g)$ is taken as a parameter. Figure A-1 shows that the coherence decreases gradually as the ratio a approaches to 1.0, and takes a minimum value at $a=1.0$. If either one of the energies of the free wave and the forced wave is much larger than that of the other, i.e. $a \gg 1$ or $a \ll 1$, the coherence is very close to unity. Moreover, it should be noted that when the parameter l/L becomes large, the coherence decreases remarkably near $a=1.0$.